Int J Clin Exp Pathol 2024;17(10):371-380
www.ijcep.com /ISSN:1936-2625/IJCEP0158605

Original Article

PCSK7, a potential target for the treatment of age-related macular degeneration: inhibition of retinal epithelial cell death

Xiaolong Zhang[1*], Xin Zhao[1*], Xiangyang Xin[2]

[1]*Department of Ophthalmology, Baogang Hospital of Inner Mongolia, Baotou 014010, Inner Mongolia, China;* [2]*Department of Ophthalmology, Baotou Central Hospital, Baotou 014040, Inner Mongolia, China.* [*]*Equal contributors.*

Received June 20, 2024; Accepted September 16, 2024; Epub October 15, 2024; Published October 30, 2024

Abstract: Background: Age-related macular degeneration (AMD) is a complex disease with a pathophysiology that remains incompletely understood. PCSK7 is closely related to the normal development of ocular tissues; however, the roles and mechanisms of PCSK7 in AMD have yet to be elucidated. Therefore, the purpose of this study was to investigate the specific manifestations of PCSK7 in AMD. Methods: An AMD cell model was established by using hydrogen peroxide (H_2O_2)-treated ARPE-19 cells. The efficiency of PCSK7 overexpression was analyzed by western blotting (WB) and quantitative reverse transcription PCR (RT-qPCR). Subsequently, a Cell Counting Kit 8 (CCK-8) assay was employed to assess the proliferation of ARPE-19 cells, while flow cytometry and immunofluorescence were utilized to examine apoptosis. Iron accumulation and glutathione (GSH) levels in cells were measured using Enzyme-linked immunosorbent assay (ELISA), and WB was conducted to evaluate the expression of anti-ferroptosis protein. Finally, JC-1 staining was performed to assess mitochondrial membrane potential. Results: Overexpressing of PCSK7 enhanced the proliferation and inhibited the apoptosis of ARPE-19 cells treated with H_2O_2. Additionally, increased PCSK7 expression suppressed intracellular iron levels and GSH content, thereby inhibiting the ferroptosis process. Furthermore, overexpression of PCSK7 restored mitochondrial membrane potential, alleviating H_2O_2-induced mitochondrial damage. Conclusions: PCSK7 might be one of the targets for the treatment of AMD through the regulation of retinal epithelial cell death.

Keywords: PCSK7, age-related macular degeneration, ARPE-19, ferroptosis, mitochondrial damage

Introduction

Age-related macular degeneration (AMD) is the leading cause of low vision and even blindness in the elderly population [1]. The clinical symptoms of AMD are distorted linear vision, the presence of a central dark spot, and reduced central vision [2, 3]. These symptoms significantly impact the health of the elderly population worldwide. AMD is a complex disease, the pathophysiology of which is not fully understood. It has been found that there is substantial cell death in the aging retina, including pyroptosis, necrotic apoptosis, and autophagy involving retinal epithelial cells [2, 4, 5].

Ferroptosis is a newly identified, iron-dependent, regulated cell death pathway. It is triggered by lipid peroxidation, characterized by iron-dependent accumulation, and is morphologically and mechanistically distinct from apoptosis and other regulated cell death pathways [6, 7]. Recent studies have found that human retinal cells with concomitant iron accumulation and lipid peroxidation could promote cell death, thereby contributing to the pathogenesis of AMD [8-10]. Therefore, reducing ferroptosis and other related cell death pathways in retinal epithelial cells is an important strategy for the treatment of AMD.

The proprotein convertases (PCs) constitute a family of nine serine-secreted proteases that regulate a wide range of biological processes in both healthy and diseased states [11]. The seventh member of this family (PC7; gene PCSK7)

https://doi.org/10.62347/LEHU9944

is a ubiquitously expressed protease with potent physiological roles. PCSK7 was involved in the regulation of lipoprotein metabolism. PCSK7-induced degradation of apoA-V inhibited the increase in adipocyte LpL activity, thereby decreasing the TG stores in adipocytes [12]. PCSK7 has been reported to be closely associated with normal eye development. For example, previous studies have shown that PCSK7 deficiency in zebrafish leads to defects in several organs, including the brain, eyes, and ear sacs [13]. In addition, PCSK7 also regulated global iron homeostasis, either by directly affecting solubility, regulating the level of expressed hemojuvenin (sHJV), which regulates iron-modulating hormones, or by maintaining iron homeostasis through the direct shedding of hTfR1, or indirectly through the activation of iron-modulating hormones [14]. However, the role of PCSK7 in AMD disease is poorly reported upon and the mechanism is not clear. Preliminary sequencing results from our group revealed that PCSK7 expression levels were significantly altered in H_2O_2-induced retinal pigment epithelial cells, suggesting that PCSK7 may be involved in the regulation of AMD.

In the present study, we found that PCSK7 inhibited oxidative stress-induced apoptosis, ferroptosis and mitochondrial damage in human retinal epithelial ARPE-19 cells. As a result, it promoted cell proliferation and ameliorates the progression of AMD.

Materials and methods

Cell culture

Human retinal pigment epithelial ARPE-19 cells were brought from American Type Culture Collection (ATCC, Manassas, VA, USA). ARPE-19 cells were grown in DMEM/F-12 medium (Gibco, New York, USA) at 37°C in a humidified environment that contained 95% air and 5% CO_2 and was supplemented with 10% FBS and 1% streptomycin/penicillin. Cells with a confluence of 80-90% were chosen for culturing and subsequent testing. Then, cells were divided into 3 groups: MOCK group (without H_2O_2 or lentivirus treatment), H_2O_2+NC group (treated with H_2O_2 and transfected with control lentiviral vector), and H_2O_2+PCSK7 group (treated with H_2O_2 and transfected with overexpressing PCSK7 lentiviral vector). Subsequently, 400 μM of hydrogen peroxide (H_2O_2, Sigma-Aldrich, St. Louis, MO, USA) was added to the cells and they were incubated for 6 h. Finally, experiments were performed with H_2O_2-treated cells.

Lentiviral infection

PCSK7 sequences were amplified using polymerase chain reaction (PCR). The PCSK7 sequence was subsequently cloned into the pCDH-CMV-MCS-EF1-copGFP vector (LV-013, GeneChem, Shanghai, China) using XbaI and EcoRI restriction enzymes to construct a PCSK7 overexpression lentiviral vector. A blank pCDH-CMV-MCS-EF1-copGFP vector, named NC, was selected for the control group. Overexpression sequences of PCSK7 are shown in the Supplementary Material. After treatment with H_2O_2, ARPE-19 cells were transfected with PCSK7 and NC lentiviral vectors in the presence of 5 g/mL polybrene (Sigma-Aldrich, St. Louis, MO, USA), and then selected after 7 days treated with puromycin (Sigma-Aldrich, St. Louis, MO, USA), with cells resistant to puromycin being isolated for further studies.

Cell Counting Kit 8 (CCK-8)

Cells from the H_2O_2-treated ARPE-19 cell line were transfected with a lentiviral vector before being placed in a 96-well plate at a density of 2000 cells/well. Then, a solution of Cell Counting Kit 8 (CCK8; Beyotime Institute of Biotechnology, Beijing, China) was added and left for 1 to 5 days. At various time points, the OD values were measured at 570 nm using a microplate reader (M2009PR, Tecan infinite, Australia).

Apoptosis detection

ARPE-19 cells transfected with PCSK7 or NC lentivirus were inoculated in 6-well plates at a density of 2×10^5 cells/well and cultured. Cells were collected and stained in Annexin-V/PE Apoptosis Assay Kit (eBioscience, Thermo Fisher Scientific, Waltham, MA, USA) for 25 minutes at room temperature and protected from light. Stained cells were analyzed for apoptosis using a FACSCanto II flow cytometer (BD Biosciences, New Jersey, USA).

Immunofluorescence

For immunofluorescence analysis, cells were cultured in 6-well plates and fixed in 4% formal-

Table 1. Antibody information

Gene name	LOT	Manufacturer	Dilution ratios
PCSK7	12044-1-AP	Proteintech	1:1000
ACSL4	ab155282	abcam	1:2000
FTH1	ab75972	abcam	1:2000
GPX4	ab125066	abcam	1:2000
Cytochrome C	ab18738	abcam	1:2000
COX IV	ab202554	abcam	1:2000
GAPDH	AF7021	Affinity	1:2000

dehyde for 30 min and permeabilized with 0.1% Triton X-100 (Sigma-Aldrich) for 10 min. The fixed cells were then blocked with 5% BSA for 30 min at room temperature and incubated overnight at 4°C with antibodies targeting PCSK7 (1:200 dilution; 12044-1-AP, Proteintech, Wuhan, China) or Caspase3 (1:200 dilution; ab208161, Abcam, Cambridge, UK). Then, cells were incubated with secondary antibody Goat Anti-mouse-FITC (S0007, Affinity, Changzhou, China) or Goat Anti-rabbit-Fluor594 (S0006, Affinity, Changzhou, China) for 1 h at 37°C and counterstained with DAPI (Sigma-Aldrich, St. Louis, MO, USA) for 10 min. The cells were then visualized under a Fluorescence microscope (Zeiss, Jena, Germany).

Enzyme-linked immunosorbent assay (ELISA)

The concentrations of glutathione (GSH, BC-1175, Solarbio Science, Beijing, China), and Iron (ab83366, Abcam, Cambridge, UK) in cells were measured via respective ELISA kits. The optical density (OD) value at 450 nm was evaluated using a microplate reader (Thermo Fisher, Waltham, MA, USA).

JC-1 assay

The mitochondrial membrane potential was detected by JC-1 assay. JC-10 kits (CA1310, Solarbio Science, Beijing, China) 1 ml were supplemented in ARPE-19 cells for 20 min at 37°C and rinsed by PBS. The cells were then visualized under a Fluorescence microscope (Zeiss, Jena, Germany) to analyze the images of the green and red fluorescence intensity in each unit. The intensity ratio of red fluorescence to green fluorescence referred to the mitochondrial membrane potential.

Detection of intracellular reactive oxygen species (ROS) accumulation

The cells were transferred to the center of a 35 mm glass-bottomed Petri dish and washed three times with 1× PBS. The samples were fixed in 4% paraformaldehyde in PBS solution for 15 minutes at room temperature. Samples were washed twice in PBS to remove residual paraformaldehyde, permeabilized with 0.5% Triton X-100 in PBS for 15 minutes, and then washed 3 times in 1× PBS. Cells were incubated with Reactive Oxygen Species Assay Kit (Solarbio Science, Beijing, China) at 37°C for 30 min, washed three times with 1× PBS, and then re-stained with DAPI for 5 min at room temperature. The staining was observed under an immunofluorescence microscope (Leica DFC500, Germany).

Quantitative reverse transcription PCR (RT-qPCR) and western blotting (WB)

For RT-qPCR, TRIzol (Sigma-Aldrich, St. Louis, MO, USA) was used to extract total RNA of cells. After the integrity was verified by electrophoresis, RNA was reversely transcribed into cDNA by Hiscript QRT supermix for qPCR (+gDNA WIPER) (Vazyme, Shanghai, China). AceQ qPCR SYBR Green master mix reagent (Vazyme, Shanghai, China) was used for qRT-PCR experiment. The primer sequence was as follow: PCSK7: F: 5'-CATTGCCTAGGTATCCGGGT-3'; R: 5'-GGGCTTCTCATGTGGCAATC-3' and GAPDH: F-5'-ATCCCATCACCATCTTCCAG-3' and R: 5'-ATGACCTTGCCCACAGCCT-3'. Relative expression was calculated using the 2-ΔCt method. GAPDH were amplified as controls for RNA integrity.

For WB, protein extraction from cells was performed by a total protein extraction kit (Goodbio Technology, Wuhan, China), and protein resolution was done on 10% Sodium dodecyl sulfate-polyacrylamide gel electrophoresis (SDS-PAGE), polyvinylidene difluoride (PVDF) membranes (Bio-Rad, California, USA) which were electroblotted. The membranes were sealed with non-fat milk, cultured with the primary antibodies (shown in **Table 1**) for one night, and then cleaned with Tris-buffered saline and Tween 20. The secondary antibody was then added and incubated for 1 hour with donkey anti-rabbit or anti-mouse IRDye-conjugated IgG (1:3000, Abcam). The images were then obtained by scanning the blots. With the aid of

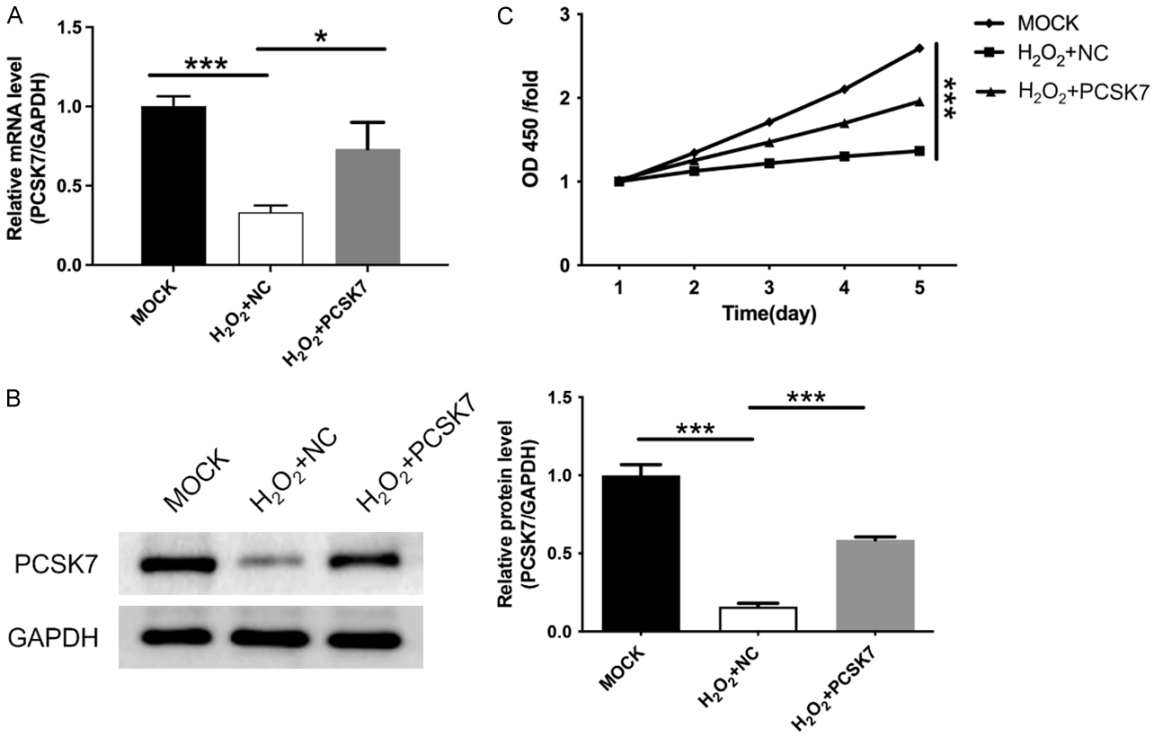

Figure 1. PCSK7 promoted proliferation in H_2O_2-induced ARPE-19 cells. A. The mRNA level of PCSK7 in H_2O_2-induced ARPE-19 infected with PCSK7 or NC were performed by RT-qPCR. B. The protein level of PCSK7 in H_2O_2-induced ARPE-19 infected with PCSK7 or NC were performed by WB. C. Cell survival in H_2O_2-induced ARPE-19 infected with PCSK7 or NC was performed by CCK8. ***P<0.001.

a very sensitive ECL chemiluminescence detection kit, the tagged protein bands were examined.

Statistical analysis

The experimental results are represented as mean ± SD from a minimum of three separate experiments. Statistical analyses were performed using GraphPad Prims (version 9.5.0) and the student's t-test was utilized to compare between the two groups. The statistical significance was set at P<0.05.

Results

PCSK7 promoted proliferation in H_2O_2-induced ARPE-19 cells

To investigate the role of PCSK7 in macular degeneration, we constructed lentiviruses overexpressing PCSK7 and transfected them into H_2O_2-treated ARPE-19 cells. Subsequently, PT-qPCR and WB assays were used to confirm the efficiency of PCSK7 overexpression. As shown in **Figure 1A**, **1B**, H_2O_2 treatment induced a decrease in PCSK7 expression, while both mRNA and protein levels of PCSK7 were elevated in cells transfected with lentivirus overexpressing PCSK7. A CCK-8 was used to probe the effect of PCSK7 on cell proliferation. We found that H_2O_2 reduced cell proliferation, whereas the overexpression of PCSK7 markedly enhanced cell proliferation in H_2O_2-induced ARPE-19 cells (P<0.001, **Figure 1C**).

PCSK7 inhibited H_2O_2-induced apoptosis in ARPE-19 cells

Flow cytometry and immunofluorescence were employed to investigate the effect of PCSK7 on apoptosis in ARPE-19 cells. The results indicated that H_2O_2 treatment led to an increase in the number of apoptotic cells, whereas the overexpression of PCSK7 reduced both the number of apoptotic cells at each time point and the overall apoptosis rate following H_2O_2 exposure (**Figure 2A**). Caspase 3, a cysteine-aspartate protease, plays a crucial role in the apoptotic process and serves as a key mediator of apoptosis. We utilized immunofluorescence to assess the expression levels of Caspase 3 in

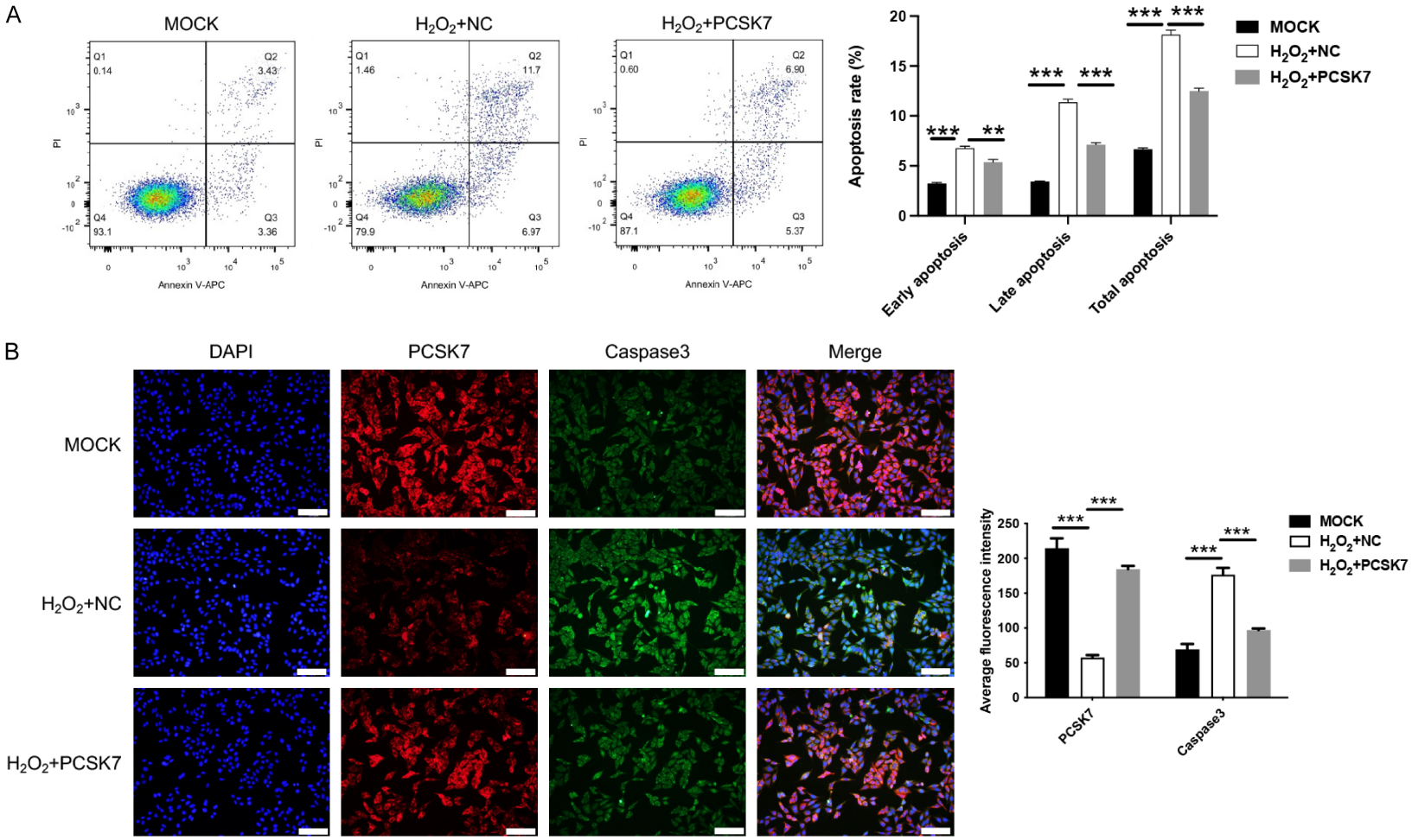

Figure 2. PCSK7 inhibited H_2O_2-induced apoptosis in ARPE-19 cells. A. Apoptosis Rate in H_2O_2-induced ARPE-19 infected with PCSK7 or NC were performed by flow cytometry. B. The expression of PCSK7 and Caspase 3 in H_2O_2-induced ARPE-19 infected with PCSK7 or NC was performed by immunofluorescence (Magnification: 200; Scale bar: 100 μm). **P<0.01, ***P<0.001.

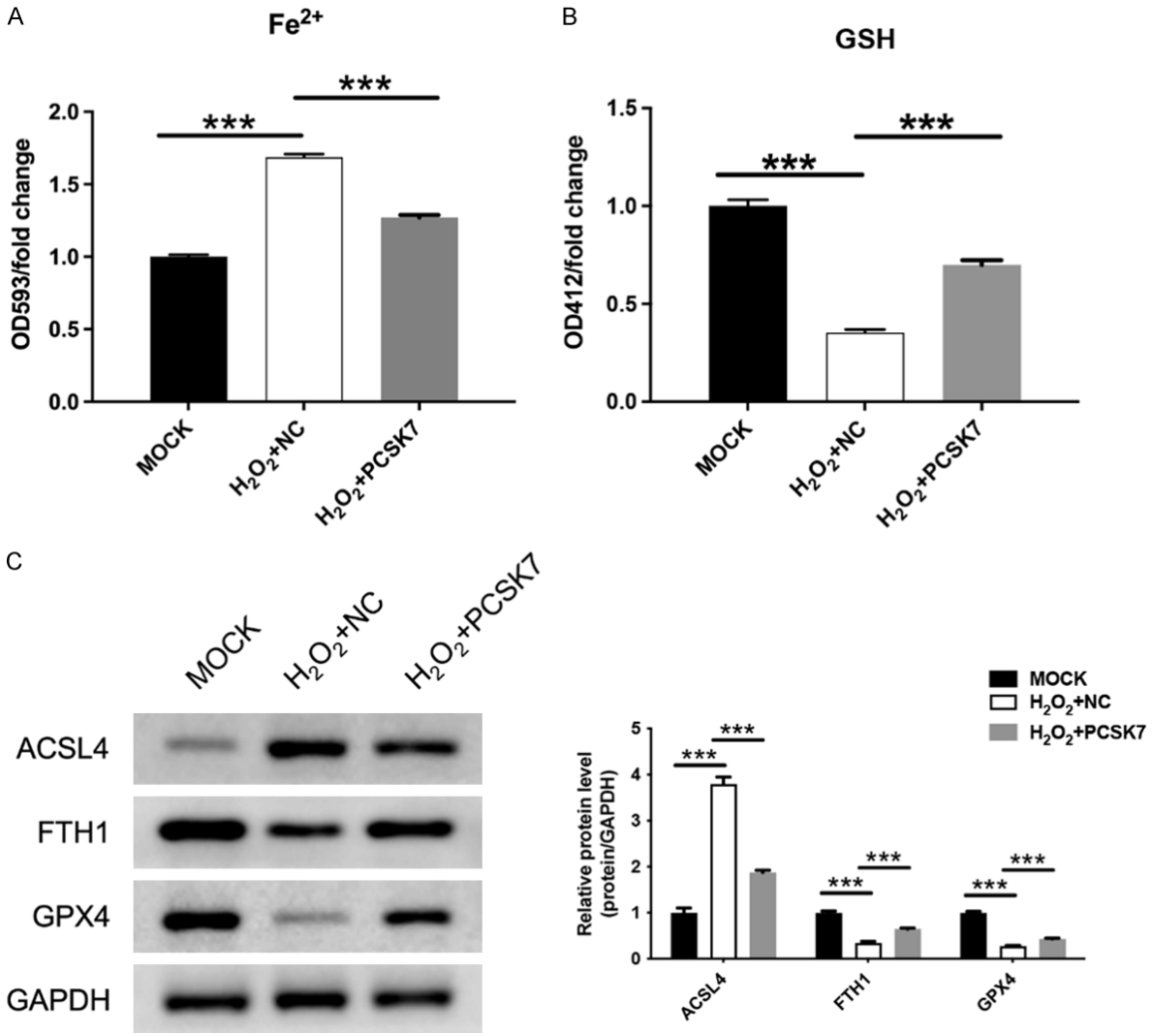

Figure 3. PCSK7 regulated ferroptosis in H_2O_2-induced ARPE-19 cells. A. Intracellular iron content in H_2O_2-induced ARPE-19 cells infected with PCSK7 or NC was performed by ELISA. B. GSH content in H_2O_2-induced ARPE-19 cells infected with PCSK7 or NC was performed by ELISA. C. The protein expression of ACSL4, FTH1, and GPX4 in H_2O_2-induced ARPE-19 infected with PCSK7 or NC was performed by WB. ***P<0.001.

ARPE-19 cells. The findings presented in **Figure 2B** demonstrated that H_2O_2 treatment enhanced the fluorescence intensity of Caspase 3, while the overexpression of PCSK7 enhanced the fluorescence intensity of PCSK7 and concurrently decreased the fluorescence intensity of Caspase 3. The above results revealed that PCSK7 expression negatively regulated cell apoptosis of ARPE-19 cells subjected to H_2O_2.

PCSK7 regulated ferroptosis in H_2O_2-induced ARPE-19 cells

Ferroptosis is a novel mode of cell death. Since ferroptosis was associated with retinal pigment epithelium (RPE) death [8], we further explored whether PCSK7 induces ferroptosis in RPE-19 cells treated with H_2O_2. Firstly, the H_2O_2-treated group exhibited increased intracellular iron content and decreased levels of glutathione (GSH) compared to the control groups. Meanwhile, overexpression of PCSK7 significantly suppressed ferrous ions (P<0.001) and enhanced GSH expression (**Figure 3A**, **3B**). Additionally, we characterized the expression of anti-ferroptosis-related proteins and found that increased expression of PCSK7 enhanced the protein expression of ACSL4, FTH1, and GPX4 (**Figure 3C**). The above results revealed that overexpression of PCSK7 inhibited ferroptosis in ARPE-19 cells treated with H_2O_2.

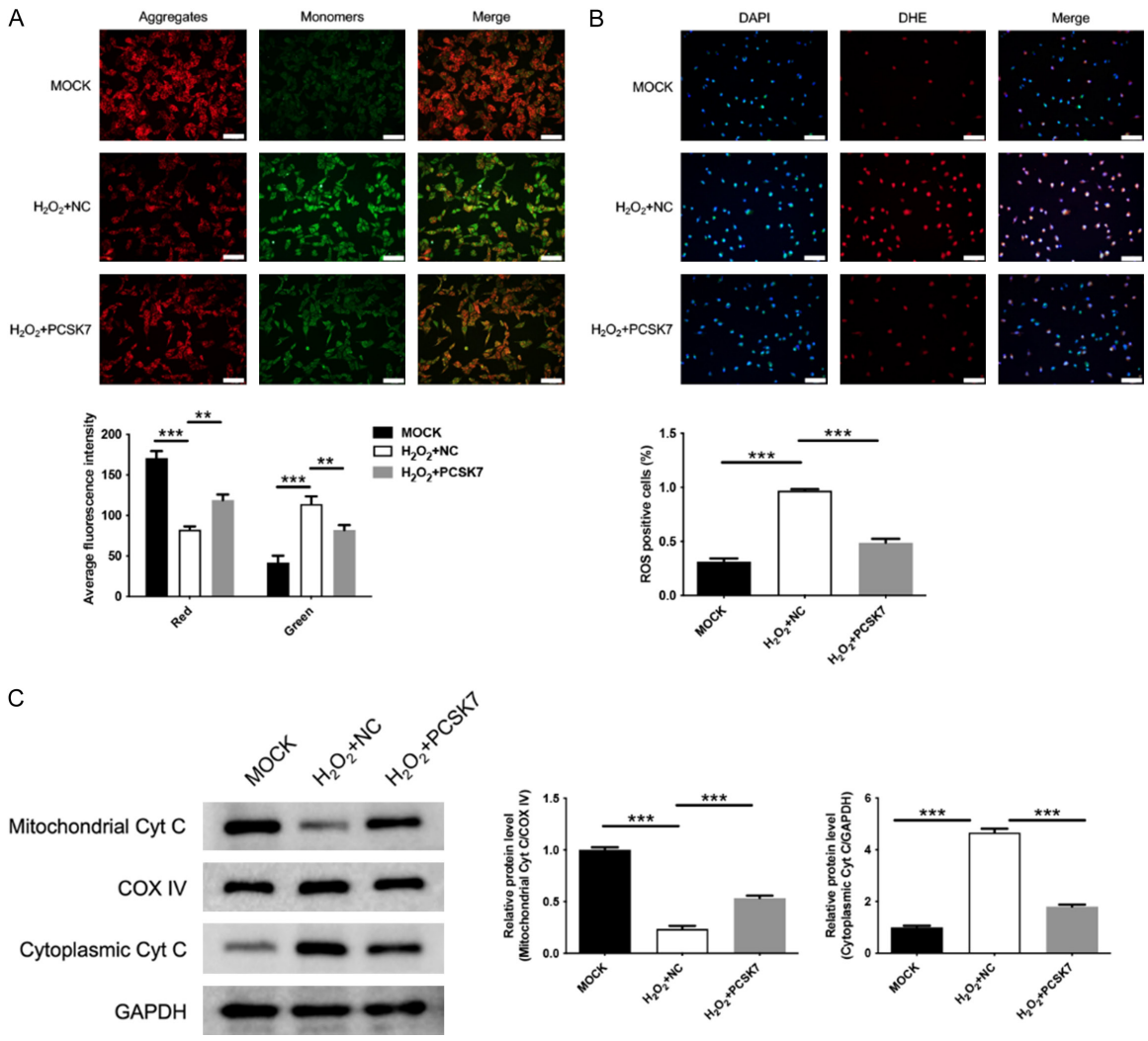

Figure 4. PCSK7 inhibited mitochondrial damage in H_2O_2-induced ARPE-19 cells. A. Mitochondrial membrane potential in H_2O_2-induced ARPE-19 infected with PCSK7 or NC was performed by JC-1 staining (Magnification: 200; Scale bar: 100 μm). B. ROS levels in H_2O_2-induced ARPE-19 infected with PCSK7 or NC were performed by IF (Magnification: 200; Scale bar: 100 μm). C. The protein expression of Cyt C in H_2O_2-induced ARPE-19 infected with PCSK7, or NC was performed by WB. **P<0.01, ***P<0.001.

PCSK7 inhibited mitochondrial damage in H_2O_2-induced ARPE-19 cells

Next, the role of PCSK7 in mitochondrial function was investigated in H_2O_2-induced ARPE-19 cells. To assess mitochondrial function, ARPE-19 cells were stained with JC-1, a dye that reflects the membrane potential of mitochondria. When the cells are healthy, they exhibit JC-1 aggregates which display red fluorescence. Conversely, when cells are damaged, the number of aggregates decreases while the number of monomers increases, resulting in green fluorescence. As shown in **Figure 4A**, the H_2O_2-induced increase in green fluorescence of JC-1 indicates heightened cellular damage. However, overexpression of PCSK7 reversed the H_2O_2-induced cellular damage, as evidenced by the red fluorescence of JC-1. Additionally, intracellular ROS levels were correlated with mitochondrial damage, so we also assayed ROS levels. The results showed that H_2O_2 increased ROS levels, while overexpression of PCSK7 mitigated this H_2O_2-induced increase in ROS (**Figure 4B**). Furthermore, WB results indicated that H_2O_2 decreased Cyt C expression in the mitochondria and increased Cyt C expression in the cytoplasm, suggesting a translocation of Cyt C from the mitochondria to the cytoplasm, indicative of mitochondrial

collapse. In contrast, overexpression of PCSK7 reversed this effect. These results suggested that overexpression of PCSK7 alleviated H_2O_2-induced mitochondrial damage in ARPE-19 cells.

Discussion

Age-related macular degeneration (AMD) is the leading cause of low vision and even blindness in the elderly population [15]. However, AMD is a complex disease whose pathophysiology is not fully understood. Persistent cell death may be a major factor contributing to the pathogenesis of AMD, in which cell necrosis is categorized into various types such as necrotic apoptosis, autophagy, pyroptosis, ferroptosis, and so on. The purpose of this study was to investigate the effect of PCSK7 on retinal epithelial cell death.

The seventh member of proprotein convertases family PCSK7 is a ubiquitously expressed protease with potent physiological roles. PCSK7 is closely related to normal development of animals, especially eye development [13], so this study constructed PCSK7 overexpression cell models to investigate its effect on AMD-related processes. Previous studies have shown that oxidative stress-mediated apoptosis was one of the mechanisms of retinal epithelial cell death [16, 17]. Exogenous H_2O_2 ultimately led to the formation and accumulation of intracellular ROS by mimicking the endogenous ROS signaling pathway, which inhibited cell growth and triggered mitochondria-dependent apoptosis [18]. As shown in this study, H_2O_2 exposure promoted apoptosis in ARPE-19 cells, while overexpression of PCSK7 suppressed the apoptosis rate of H_2O_2-induced ARPE-19 cells and reduced the expression of the apoptosis regulator Caspase 3. This result suggested that PCSK7 might exert anti-AMD effects by inhibiting oxidative stress-induced apoptosis in retinal epithelial cells.

In addition to exploring the apoptotic effects of PCSK7 on ARPE-19 cells, we also explored other cell death types like ferroptosis. Ferroptosis is characterized by the iron-dependent accumulation of lipid ROS and is morphologically and mechanistically distinct from apoptosis or other programmed cell death pathways [7, 19, 20]. With age, the retinal epithelium leads to an increase in oxidative stress [9], which in turn leads to the accumulation of iron, a hallmark of AMD. In this study, we found that H_2O_2 induced iron accumulation and inhibited the expression of anti-ferroptosis proteins, which was reversed by overexpression of PCSK7. Interestingly, previous studies have found that PCSK7can regulate global iron homeostasis [14], and our results confirm the previous studies.

Under oxidative stress, overproduction of intracellular ROS leads to mitochondrial dysfunction and increases mitochondrial membrane permeability, resulting in depolarization of the mitochondrial membrane potential as well as release of cytochrome c from the mitochondria into the cytoplasm [21, 22]. The lack of mitochondrial function also contributes to the massive death of retinal epithelial cells and is associated with early AMD [23, 24]. The results of the present study showed that H_2O_2 induced a collapse of the mitochondrial membrane potential in ARPE-19 cells, resulting in mitochondrial damage, which was alleviated by overexpression of PCSK7.

This study has a few limitations. On one hand, we have not demonstrated the death-regulating effect of PCSK7on retinal epithelial cells in an animal model; on the other hand, the specific molecular mechanism by which PCSK7 regulates cell death had not been elucidated in detail. Therefore, the focus of the next study needs to further elucidate the role of PCSK7on the pathogenesis of AMD in vivo, and the effect of PCSK7on downstream signaling pathways which may regulate cell death.

In conclusion, the present study found that PCSK7 inhibited oxidative stress-induced apoptosis, ferroptosis and mitochondrial damage in human retinal epithelial ARPE-19 cells, thereby promoting cell proliferation and ameliorating the AMD progression. PCSK7 might be one of the targets for the treatment of AMD through the regulation of retinal epithelial cell death.

Acknowledgements

This work was supported by the Baotou Health Science and Technology Program (wsjkkj2022-091).

Disclosure of conflict of interest

None.

Address correspondence to: Xiangyang Xin, Department of Ophthalmology, Baotou Central Hospital, No. 61, Huan Cheng Road, Donghe District, Baotou 014040, Inner Mongolia, China. Tel: +86-15049249969; E-mail: xinxiangyang_2006@163.com

References

[1] Balaratnasingam C and Curcio CA. Biomarkers in age-related macular degeneration. Clin Exp Ophthalmol 2024; 52: 384-386.

[2] Guymer RH and Campbell TG. Age-related macular degeneration. Lancet 2023; 401: 1459-1472.

[3] Flores R, Carneiro Â, Vieira M, Tenreiro S and Seabra MC. Age-related macular degeneration: pathophysiology, management, and future perspectives. Ophthalmologica 2021; 244: 495-511.

[4] Lewis Luján LM, McCarty MF, Di Nicolantonio JJ, Gálvez Ruiz JC, Rosas-Burgos EC, Plascencia-Jatomea M and Iloki Assanga SB. Nutraceuticals/drugs promoting mitophagy and mitochondrial biogenesis may combat the mitochondrial dysfunction driving progression of dry age-related macular degeneration. Nutrients 2022; 14: 1985.

[5] Chen M, Rong R and Xia X. Spotlight on pyroptosis: role in pathogenesis and therapeutic potential of ocular diseases. J Neuroinflammation 2022; 19: 183.

[6] Tang D, Chen X, Kang R and Kroemer G. Ferroptosis: molecular mechanisms and health implications. Cell Res 2021; 31: 107-125.

[7] Liang D, Minikes AM and Jiang X. Ferroptosis at the intersection of lipid metabolism and cellular signaling. Mol Cell 2022; 82: 2215-2227.

[8] Henning Y, Blind US, Larafa S, Matschke J and Fandrey J. Hypoxia aggravates ferroptosis in RPE cells by promoting the Fenton reaction. Cell Death Dis 2022; 13: 662.

[9] Zhao T, Guo X and Sun Y. Iron accumulation and lipid peroxidation in the aging retina: implication of ferroptosis in age-related macular degeneration. Aging Dis 2021; 12: 529-551.

[10] Wei TT, Zhang MY, Zheng XH, Xie TH, Wang W, Zou J, Li Y, Li HY, Cai J, Wang X, Tan J, Yang X, Yao Y and Zhu L. Interferon-γ induces retinal pigment epithelial cell ferroptosis by a JAK1-2/STAT1/SLC7A11 signaling pathway in age-related macular degeneration. FEBS J 2022; 289: 1968-1983.

[11] Cendron L, Rothenberger S, Cassari L, Dettin M and Pasquato A. Proprotein convertases regulate trafficking and maturation of key proteins within the secretory pathway. Adv Protein Chem Struct Biol 2023; 133: 1-54.

[12] Ashraf Y, Duval S, Sachan V, Essalmani R, Susan-Resiga D, Roubtsova A, Hamelin J, Gerhardy S, Kirchhofer D, Tagliabracci VS, Prat A, Kiss RS and Seidah NG. Proprotein convertase 7 (PCSK7) reduces apoA-V levels. FEBS J 2020; 287: 3565-3578.

[13] Turpeinen H, Oksanen A, Kivinen V, Kukkurainen S, Uusimäki A, Rämet M, Parikka M, Hytönen VP, Nykter M and Pesu M. Proprotein convertase subtilisin/kexin type 7 (PCSK7) is essential for the zebrafish development and bioavailability of transforming growth factor β1a (TGFβ1a). J Biol Chem 2013; 288: 36610-36623.

[14] Schwienbacher C, Serafin A, Zanon A, Pramstaller PP, Pichler I and Hicks AA. Involvement of proprotein convertase PCSK7 in the regulation of systemic iron homeostasis. Hepatology 2013; 58: 1860-1861.

[15] Mitchell P, Liew G, Gopinath B and Wong TY. Age-related macular degeneration. Lancet 2018; 392: 1147-1159.

[16] Yang YC, Chien Y, Yarmishyn AA, Lim LY, Tsai HY, Kuo WC, Tsai PH, Yang SH, Hong SI, Chen SJ, Hwang DK, Yang YP and Chiou SH. Inhibition of oxidative stress-induced epithelial-mesenchymal transition in retinal pigment epithelial cells of age-related macular degeneration model by suppressing ERK activation. J Adv Res 2024; 60: 141-157.

[17] Harju N. Regulation of oxidative stress and inflammatory responses in human retinal pigment epithelial cells. Acta Ophthalmol 2022; 100 Suppl 273: 3-59.

[18] He Y, Zheng Z, Liu C, Li W, Zhao L, Nie G and Li H. Inhibiting DNA methylation alleviates cisplatin-induced hearing loss by decreasing oxidative stress-induced mitochondria-dependent apoptosis via the LRP1-PI3K/AKT pathway. Acta Pharm Sin B 2022; 12: 1305-1321.

[19] Liu J, Kang R and Tang D. Signaling pathways and defense mechanisms of ferroptosis. FEBS J 2022; 289: 7038-7050.

[20] Niu B, Liao K, Zhou Y, Wen T, Quan G, Pan X and Wu C. Application of glutathione depletion in cancer therapy: enhanced ROS-based therapy, ferroptosis, and chemotherapy. Biomaterials 2021; 277: 121110.

[21] Rehfeldt SCH, Laufer S and Goettert MI. A highly selective in vitro JNK3 inhibitor, FMU200, restores mitochondrial membrane potential and reduces oxidative stress and apoptosis in SH-SY5Y cells. Int J Mol Sci 2021; 22: 3701.

[22] Zaib S, Hayyat A, Ali N, Gul A, Naveed M and Khan I. Role of mitochondrial membrane potential and lactate dehydrogenase A in apoptosis. Anticancer Agents Med Chem 2022; 22: 2048-2062.

[23] Cano M, Datta S, Wang L, Liu T, Flores-Bellver M, Sachdeva M, Sinha D and Handa JT. Nrf2 deficiency decreases NADPH from impaired IDH shuttle and pentose phosphate pathway in retinal pigmented epithelial cells to magnify oxidative stress-induced mitochondrial dysfunction. Aging Cell 2021; 20: e13444.

[24] Park Y, Jeong Y, Son S and Kim DE. AMPK-induced mitochondrial biogenesis decelerates retinal pigment epithelial cell degeneration under nutrient starvation. BMB Rep 2023; 56: 84-89.

Supplementary Material

Sequence of the gene overexpressing PCSK7

ATGCCGAAGGGGAGGCAGAAAGTGCCACACTTGGATGCCCCCCTGGGCCTGCCCACCTGCCTCTGGCTGGA-
ATTAGCCGGGCTCTTCTTACTGGTTCCCTGGGTCATGGGCCTGGCAGGGACAGGTGGGCCTGATGGCCA-
GGGCACAGGGGGGCCGAGCTGGGCTGTGCACCTGGAAAGCCTGGAAGGTGACGGGGAGGAAGAGA-
CTCTGGAGCAGCAGGCGGATGCCTTGGCCCAGGCAGCAGGGCTGGTGAATGCTGGACGCATCGGAG-
AGCTTCAGGGGCACTACCTCTTTGTCCAGCCTGCTGGGCACAGGCCGGCCCTGGAGGTGGAGGCCAT-
CCGGCAGCAGGTGGAGGCTGTGTTGGCTGGGCATGAAGCTGTGCGCTGGCACTCAGAGCAGAGGCTGCT-
AAGGCGGGCCAAGCGCAGCGTCCACTTCAACGACCCCAAGTACCCGCAGCAATGGCACCTGAATAAC-
CGACGGAGCCCGGGCAGGGACATCAACGTGACGGGTGTGTGGGAACGCAATGTGACTGGGCGAGGGGT-
GACGGTGGTGGTAGTGGATGACGGAGTGGAACACACCATCCAGGACATTGCACCCAACTATAGCCC-
TGAGGGTAGCTATGACCTCAACTCTAATGACCCTGACCCCATGCCCCACCCGGATGTGGAGAATGGCAACCA-
CCATGGCACGCGATGTGCAGGAGAGATCGCGGCTGTGCCCAACAACAGCTTCTGTGCCGTGGGCG-
TGGCCTACGGGAGCCGCATCGCAGGTATCCGGGTACTGGATGGACCTCTCACAGACAGCATGGAGGCAGTG-
GCGTTCAACAAGCACTATCAGATCAATGACATCTACAGCTGCAGCTGGGGACCAGATGACGATG-
GGAAGACAGTGGATGGCCCCCATCAGCTTGGAAAGGCTGCCTTACAACATGGGGTGATTGCTGGTCGCCAGGG-
CTTTGGGAGCATCTTTGTGGTAGCCAGTGGCAACGGAGGCCAACACAACGACAACTGCAACTACGAT-
GGCTACGCCAACTCCATCTACACCGTCACCATAGGAGCTGTGGATGAGGAGGGACGCATGCCTTTCTATGCA-
GAAGAATGTGCCTCCATGCTGGCAGTCACCTTCAGTGGTGGGGACAAGATGCTTCGGAGCATTGT-
GACCACTGACTGGGACCTTCAGAAGGGCACTGGCTGCACTGAGGGCCACACAGGGACCTCAGCTGCAGCGCCT-
CTGGCAGCTGGCATGATAGCCTTAATGCTGCAGGTGCGGCCCTGCCTCACGTGGCGTGACGTCC-
AGCACATCATTGTCTTCACAGCCACCCGGTATGAGGATCGCCGTGCAGAGTGGGTCACCAACGAGGCAGGCTTC-
AGCCATAGCCACCAGCACGGTTTCGGCCTCCTCAACGCCTGGAGGCTCGTGAATGCAGCCAAGATC-
TGGACATCTGTCCCTTACTTAGCATCCTACGTCAGTCCCGTGTTAAAAGAAAACAAGGCGATTCCGCAGTCCC-
CCCGTTCCCTGGAGGTCCTGTGGAATGTCAGCAGGATGGACCTGGAGATGTCAGGGCTGAAGAC-
CCTGGAGCATGTGGCAGTGACAGTCTCCATCACTCACCCACGGCGCGGCAGCTTGGAGCTGAAGCTGTTCTGC-
CCCAGTGGCATGATGTCCCTCATCGGCGCCCCCCGCAGCATGGACTCGGATCCCAACGGCTTCA-
ATGACTGGACCTTCTCCACTGTGCGATGCTGGGGGGAGAGAGCCCGAGGGACCTACAGGCTTGTCATCAGGG-
ATGTCGGGGATGAGTCATTCCAGGTCGGCATCCTCCGGCAATGGCAGCTGACCCTATATGGCTCTG-
TGTGGAGTGCAGTAGACATCAGGGACAGACAAAGGCTGTTAGAGAGTGCCATGAGTGGAAAATACCTGCAC-
GATGACTTCGCCCTGCCCTGCCCACCGGGGCTGAAAATTCCTGAGGAAGATGGTTACACCATCACCC-
CCAACACCCTCAAGACCCTGGTGCTGGTAGGCTGTTTCACCGTCTTCTGGACTGTTTACTACATGCTGGAAGTAT-
ATTTGAGCCAGAGGAATGTGGCTTCCAATCAAGTTTGTAGGAGTGGACCCTGCCACTGGCCCCATC-
GGAGCCGGAAAGCCAAGGAGGAAGGGACAGAGCTAGAATCAGTGCCACTTTGCAGCAGCAAGGATCCAGAC-
GAAGTGGAAACAGAGAGCAGGGGCCCTCCCACCACCTCTGACCTCCTTGCCCCAGACCTGCTGGAG-
CAAGGGGACTGGAGCCTGTCCCAGAACAAGAGCGCCCTGGACTGCCCTCATCAGCACCTAGACGTACCGCA-
CGGGAAGGAGGAGCAGATCTGCTGA